

Generating sub-TeV quasi-monoenergetic proton beam by an ultra-relativistically intense laser in the snowplow regime

F.L.Zheng,^{1,2} H.Y.Wang,¹ X.Q.Yan,^{1,3,*} J.E.Chen,¹ Y.R.Lu,¹ Z.Y.Guo,¹ T.Tajima,⁴ and X.T.He^{1,†}

¹*Center for Applied Physics and Technology, State Key Laboratory of Nuclear Physics and Technology, Peking University, Beijing 100871, China*

²*Graduate School, China Academy of Engineering Physics, P.O. Box 8009, Beijing 100088, Peoples Republic of China*

³*Institute of Applied Physics and Computational Mathematics, P. O. Box 8009, Beijing 100088, China*

⁴*Fakultät f. Physik, LMU München, D-85748 Garching, Germany*

(Dated: March 2, 2022)

Snowplow ion acceleration is presented, using an ultra-relativistically intense laser pulse irradiating on a combination target, where the relativistic proton beam generated by radiation pressure acceleration can be trapped and accelerated by the laser plasma wakefield. The theory suggests that sub-TeV quasi-monoenergetic proton bunches can be generated by a centimeter-scale laser wakefield accelerator, driven by a circularly polarized (CP) laser pulse with the peak intensity of 10^{23} W/cm² and duration of 116fs.

PACS numbers: 52.38.Kd, 41.75.Jv, 52.35.Mw, 52.59.-f

Laser-driven ion acceleration has drawn attention for many applications, e.g., proton cancer therapy[1], fast ignition of thermonuclear fusion by protons [2], conversion of radioactive waste [3], high energy physics accelerator [4] and astrophysics [5]. All these applications may be enabled by the introduction of near-future high-intensity lasers (i.e. ELI), which will be capable of producing pulses with intensity $10^{22} - 10^{24}$ W/cm² [6].

Radiation Pressure Acceleration (RPA)[7] accelerates ions efficiently and theoretical studies show that GeV proton beam may be generated by an ultra-intense laser with intensities above 10^{22} W/cm² [8, 10, 11]. Although the acceleration field is over tens TeV/m, the acceleration length is normally shorter than hundreds microns. Because of the energy scaling, it is difficult to further increase the ion to very high energies (i.e. TeV). Quasi-monoenergetic GeV electron beam can be generated by a centimeter-scale laser plasma wakefield accelerator(LPWA) [12]; however, it is not easy to capture and continuously accelerate the nonrelativistic ions. Shen et al.[13] reports a laser pulse with an ultrarelativistic intensity can excite an electrostatic field, which can capture protons from underdense plasma and accelerate them to tens GeV. Recently Yu et al. [14] found that the underdense gas behind a thin foil can accelerate the proton beam to 60GeV by driving high-amplitude electrostatic fields moving at a high speed. There is an important question whether it is possible to generate TeV-level proton beams by the laser plasma wakefield accelerator.

This letter reports an ultra-relativistically intense laser can excite the plasma wakefield that traps the relativistic proton beam and accelerates it over a few centimeters. An analytic model is derived for proton acceleration that extends the applicability of Esarey's classic plasma wakefield theory [15] and has been confirmed by our PIC simulations. Our scaling law shows that sub-TeV

quasi-monoenergetic proton bunches can be generated by a circularly polarized (CP) laser pulse with the intensity of 10^{23} W/cm² and duration of 116 fs. A combined target in Fig.1 (a) shows a planar hydrogen target that is followed by underdense heavy-ion background gas with a charge-to-mass ratio of 1/3. When the foil thickness D is equal to $\frac{1}{2\pi} \frac{n_c}{n_e} a_0 \lambda_l$, a mono-energetic proton beam is generated from a moving double layer [14], Fig.2(a) suggests that protons and electron layer are very close. The relativistic protons can quickly overrun the laser front that results in shorter dephasing length and lower proton energy. If a thinner foil satisfies

$$l_0 < D < \frac{1}{2\pi} \frac{n_c}{n_e} a_0 \lambda_l, \quad (1)$$

the ponderomotive force quickly pushes electrons to the rear of the foil (see Fig.2(b)), the electrons that are piled up there reaches density far greater than γn_c . Meanwhile protons in the foil are accelerated by the separated charge field. Here l_0, n_e, n_c , and λ_l are the plasma skin depth, plasma density, critical plasma density, and laser wavelength, respectively. $a_0 = eA/m_e \omega_l c$ is the normalized laser amplitude and A is the laser vector potential. $\gamma = (1 + I \lambda_l^2 / 1.37 \times 10^{18})^{1/2}$, I is laser intensity, λ_l in units of micron. The electron-layer in rear of the foil is pushed out of the foil by the laser pulse soon before double-layer (consists of electrons and protons) is formed. The layer runs in the lower density gas and is further pushed by the laser pulse like light-sail to generate "Snow-plow" effects on enhancement of electron number. The electrons in gas plasma drew away from the foil generate a large electric field, then the protons that have been accelerated to GeV level start long march in gas by the wakefield acceleration. This acceleration scheme is named the snowplow regime. We also notice a connection of the above plasma acceleration with "snowplow" acceleration in Ref. [16]. In order to grasp the main physics and to construct a

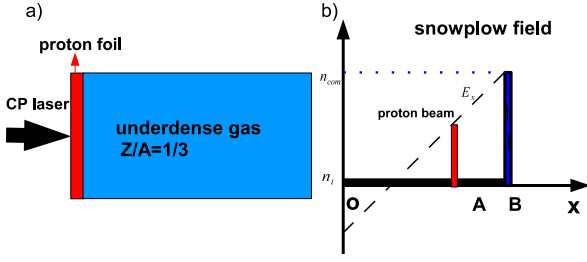


FIG. 1: (color online)(a)Acceleration scheme, the initial density of the hydrogen foil $n_0/n_c = 20$, thickness $D = 0.5\lambda_l$; the plasma density of the tenuous gas $n_e/n_c = 0.01$, the length of the gas plasma is $12000\lambda_l$; (b)Sketch map for the snowplow process, the dynamical density of ions is n_i and electron density in the snowplow layer is n_{com} . The position B indicates the laser pulse front and A is an arbitrary point for calculating the local electrostatic field in the snowplow region.

physical model, in this letter one-dimensional(1D) theory is derived and testified by 1D and 2D PIC simulations.

Considering the classic 1D plasma wakefield driven by a laser pulse [15], two typical features should be noticed in the ultra-relativistic intensity: (i)Lengthening of the plasma wavelength $l_s = (\gamma n_c/n_e)^{1/2}\lambda_l$; (ii)Enhancement of the nonlinear wavebreaking field $E_B = 3\pi(\gamma n_e/n_c)^{1/2}E_0$, where the critical plasma density $n_c = \pi m_e c^2/e^2\lambda_l^2$. The highly nonlinear wakefield wavelength l_s and wavebreaking field E_B are increased by a factor of $\gamma^{1/2}$ over the non-relativistic version, where the electric field strength is normalized by $E_0 = m_e\omega_l c/e$. In this regime we adopt a CP laser pulse with a wavelength $\lambda_l = 1\mu m$ and a peak intensity $I_0 = 1.7125 \times 10^{23} W/cm^2$, corresponding to peak dimensionless laser amplitude $a_0 = 250$. When the foil thickness D satisfies Eq.(1), the relativistic protons can be captured by the excited wakefield in the underdense gas and be stably accelerated in the snowplow regime over a long distance. An analytic model is developed to estimate the acceleration field, dephasing length, pump depletion length, and maximum proton energy. The acceleration length in snowplow regime is proportional to $a_0^{3/2}$ and maximum proton energy scales with a_0^2 . It shows that sub TeV monoenergetic proton beam is generated in the laser intensity of $10^{23} W/cm^2$. To our best knowledge, it is the best efficient proton acceleration mechanism in terms of acceleration length and maximum energy.

First we carried out simulation using a fully relativistic particle-in-cell code (KLAP) [8, 9]. The laser pulse has a trapezoidal shape longitudinally with $15\lambda_l$ flat top and $20\lambda_l$ ramp on the rise side. The ramp profile is $a = a_0 \sin^2(\pi t/40)$. At time $t=0$ it is normally incident from the left on a uniform, fully ionized hydrogen foil of the thickness $D = 0.5\mu m$ and normalized density

$N = n_0/n_c = 20$. Behind the hydrogen foil is the tenuous heavy-ion-gas with a charge-to-mass ratio of $1/3$ and a plasma density of $n_e = 0.01n_c$. Here the simulation box has a size of $12000\lambda_l$ in x plane and a space resolution of 20 cells/ λ_l . Each cell is filled with 10 macroparticles for gas plasma and 20000 macroparticles for foil plasma. The initial electron and ion temperature are $0.1eV$.

After the proton beam is accelerated to GeV level in the laser foil interactions, the laser pulse passes through the foil and piles electrons in the underdense gas plasma as Fig.1 (b) shows, which is one of most important and remarkable features in the snowplow regime. Here the electron layer and the positive electrostatic field are called the snowplow layer and snowplow field, respectively. The snowplow layer can continuously trap electrons in the snowplow process, so the acceleration field exists stably for a long distance. In the snowplow region, it is found that the length of the snowplow region is equal to $l_s = (\gamma n_c/n_e)^{1/2}\lambda_l$ and the snowplow velocity approximately equals to the group velocity of laser pulse in the underdense plasma. First we estimate the electrostatic field E_A at an arbitrary point x_A in the snowplow region. The component from ions is $E'_A = 4\pi en_i x_A - 4\pi en_i (l_s - x_A)$. The contribution from the snowplow layer at position x_A is $E''_A = \frac{4\pi en_e l_s}{2}$. The longitudinal electrostatic field at x_A is $E_A = E'_A + E''_A = 4\pi en_e (2x_A - l_s/2)$. Therefore, the maximum snowplow field at the laser front x_B is

$$E_B = 3\pi(\gamma n_e/n_c)^{1/2}E_0. \quad (2)$$

Since the injected GeV protons are still slower than the laser pulse at the beginning, the ion beam should be injected into the front side of snowplow region. Afterwards protons are gradually accelerated and overrun the laser pulse (see Fig.4(a)). The optimized distance between injected proton beam and laser pulse front is defined by l_{inj} . It is approximately $\frac{1}{4}l_s$ in our simulation. Once the proton beam is injected into the wakefield, its maximum energy depends on the laser pump depletion length and proton dephasing length. The laser pump depletion length L_{pd} is estimated [15]: $E_x^2 \cdot L_{pd} \simeq E_l^2 \cdot L_l$, where E_x is the longitudinal electrostatic field driven by laser pulse in the snowplow wakefield and L_l is the length of laser pulse. Assuming the group velocity of laser pulse is extremely close to light velocity in free space, pump depletion length can be defined as

$$L_{pd} \simeq \frac{L_l}{v_{etch}} \cdot c, \quad (3)$$

where v_{etch} is the depletion velocity of laser pulse. The etching velocity of laser pulse reads $v_{etch} \simeq \frac{9\pi^2 n_e}{a_0 n_c} c$. It shows the etching velocity of laser pulse scales as n_e/a_0 .

The dephasing length of proton is given approximately by $L_{dp} \simeq \frac{l_{inj}}{v_p - (v_g - v_{etch})} \cdot v_p$, where l_{inj} is the injected length between proton beam and laser pulse front, v_g is the laser group velocity, v_p is the proton velocity. It

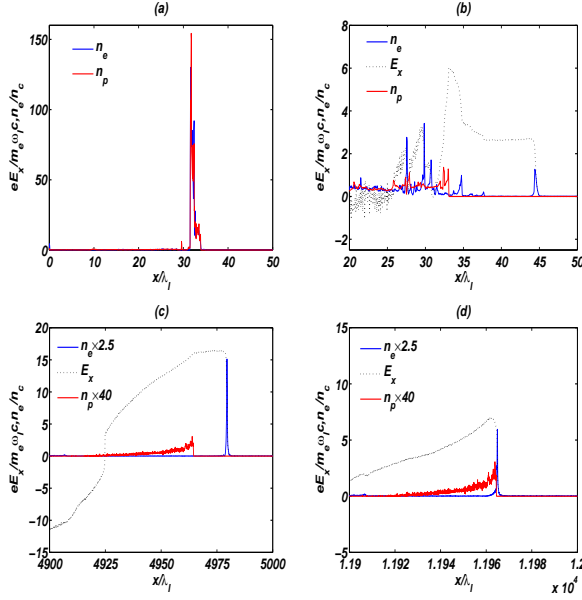


FIG. 2: (Color online) Electron density n_e/n_c (blue solid line), proton density n_p/n_c (the red solid line) and longitudinal electrostatic field $eE_x/m_e\omega_L c$ (the black dashed line). (a) When $D = \frac{1}{2\pi} \frac{n_c}{n_e} a_0 \lambda_l$ double-layer is formed at $t=50T_L$. When $D=0.5\mu m$ snapshots are taken at time (b) $50T_L$, (c) $5000T_L$, (d) $12000T_L$.

can be further simplified when both v_g and v_p are very close to light speed, which means $v_{etch} \gg (v_p - v_g)$. The proton dephasing length is:

$$L_{dp} \simeq \frac{1}{36\pi^2} (a_0 n_c / n_e)^{3/2} \lambda_l. \quad (4)$$

In case of $L_l > \frac{1}{4} (a_0 n_c / n_e)^{1/2} \lambda_l$ the laser pump depletion length is greater than the dephasing length, the maximum energy proton beam can be given as

$$W_{max} \simeq \frac{1}{6} (a_0^2 n_c / n_e) m_e c^2. \quad (5)$$

It implies that the maximum proton energy in the snowplow regime scales with a_0^2 and n_e^{-1} . This is quite an efficient acceleration scaling law.

The snapshots of electron density, proton density, and electrostatic field are plotted in Fig.2. The proton beam has been continuously accelerated until laser pulse is completely depleted at $t=12000T_L$. When the proton beam approaches the laser front, the beam loading causes a substantial reduction of the electrostatic field as shown in Fig.2(c) and 2(d). The theoretical values of the longitudinal electrostatic field $E_x = 14.9$ in the unit of E_0 , the dephasing length $l_{pd} = 11125\mu m$, the maximum energy of proton beam $W_{max} = 532$ GeV and the etching velocity $v_{etch} = 0.0036c$, respectively. They are consistent with the simulation results. Fig.3 shows the energy spread (FWHM) of the beam is less than 20%. The maximum proton energy and averaged one are 540GeV

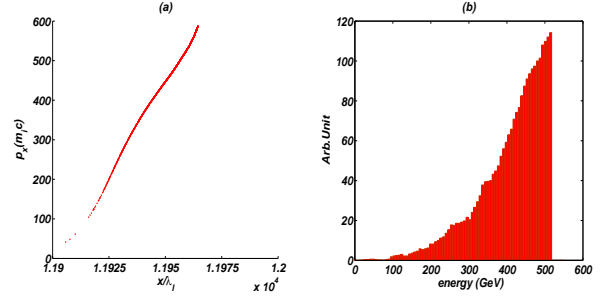


FIG. 3: (Color Online) Longitudinal phase space for protons $p_x/m_i c$ (a) and energy spectrum of trapped protons (b) from simulations at $t=12000T_L$.

and 437GeV, respectively. There are 1.72% of the total protons located inside this energy window. The proton beam is compressed in the phase space and the final quasi-monoenergetic beam is shorter than $100\mu m$.

As Fig.4(a) shows, proton beams move backward with respect to the snowplough reference since the laser group velocity is greater than the proton beam. As a result, the distance between proton beam and laser front increases to reach the maximum l_{inj} in the initial injection stage. Later it begins to decrease due to the erosion of the laser pulse front. The slopes of the solid lines represent the etching velocities of the laser pulse for different gas densities. The maximum longitudinal electrostatic field, dephasing length, and maximum proton energy are plotted versus the density in Fig.4(b,c,d). It shows the maximum energy of the proton beam is increasing with plasma density decreasing. The dotted lines indicate that the pulse depletion length is shorter than the dephasing length if the plasma density is smaller than $0.01n_c$. In order to increase the proton energy, we may increase the intensity of laser pulse and reduce the gas density, which can increase both the dephasing length and pump depletion length.

The density ranges over more than three orders of magnitude in 1D simulations, it is difficult to do a full scale 2D simulations (e.g. TeV protons). A small simulation box $40 \times 1000 \lambda_l^2$ is chosen with a spatial resolution of 5 cells/ λ_l in y plane and 20 cells/ λ_l in x plane. Each cell contains 4 particles for each species of gas plasma, 400 particles for foil plasma. The foil is the same as in 1D simulations while the gas density is $0.2n_c$. The laser pulse is temporally and transversely super-Gaussian, $I = I_0 \exp(-(r/r_0)^4 - [(t - t_0)/\tau]^8)$, where $r_0 = 10\mu m$, $t_0 = 55$ fs, and $\tau = 55$ fs are taken. Fig.5 shows the snowplow layer, electrostatic field, and phase space are similar with 1D results while the maximum proton energy reaches 50GeV that agrees with 1D simulations. Since protons gain energy mainly from the electrostatic field [14], the return current and magnetic field in 2D simulations are not important for proton acceleration. Furthermore, the lost fraction of electrons in snowplow

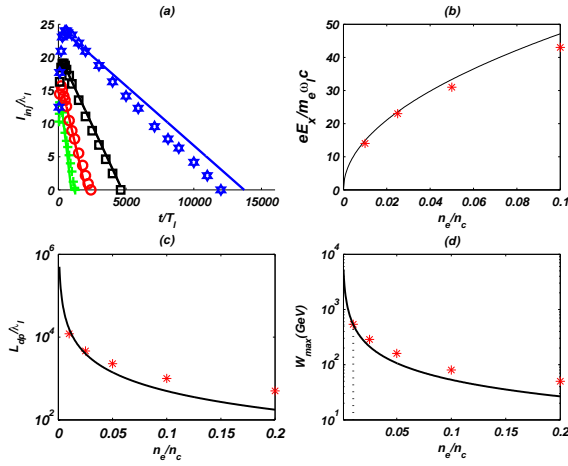


FIG. 4: (Color Online)(a)Distance between proton beam and the laser pulse front. It varies with time for different gas densities, where blue, black, red and green curves represent the gas densities of $0.01n_c$, $0.025n_c$, $0.05n_c$ and $0.1n_c$, respectively; (b)Longitudinal electrostatic field $eE_x/m_e\omega_l c$;(c)Dephasing length; (d) Maximum proton energy. Here the solid lines are theoretical curves and simulation results are marked by different symbols(e.g. star,diamond and squire).

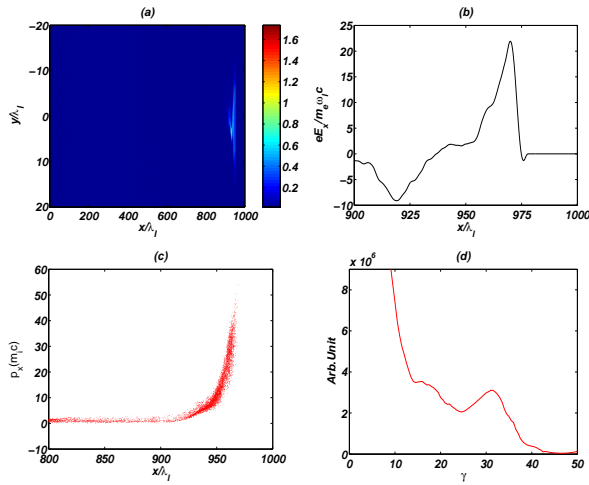


FIG. 5: (Color Online)2D simulation results at $t=990 T_l$.(a)Electron density distribution; (b)Electrostatic field on the axis ;(c)Proton phase space; (d)Proton spectrum.

layer can be compensated from gas plasma and snowplow layer is still kept at the end of simulations. The disadvantageous multi-dimensional effects (e.g. hole boring, Rayleigh-Taylor instability) in laser foil interactions [7] are not observed in our simulations. These effects lead to very stable proton acceleration in the multi-dimensional situation.

In conclusion, snowplow ion acceleration, using an ultra-relativistically intense laser pulse irradiating on the combination target, is presented. A 1D model that can

predict the proton dephasing length, pump depletion length, and maximum proton energy is derived, which is verified by 1D and 2D PIC simulations. It shows that sub-TeV quasi-monoenergetic proton bunches can be generated by a centimeter-scale laser wakefield accelerator, excited by a laser pulse with the intensity of $10^{23}\text{W}/\text{cm}^2$ and duration of 116fs. The final proton beam is shorter than $100\ \mu\text{m}$ and may be used to excite the plasma wakefield to accelerate electrons to hundreds GeV, as Cadwell proposed [17].

We thank G.Mourou, Z.M.Sheng, C.T.Zhou, C. Y. Zheng, H. Zhang, B. Liu, and H.C.Wu for useful discussions and help.This work was supported by National Nature Science Foundation of China (Grant Nos. 10935002,10835003,11025523) and National Basic Research Program of China (Grant No. 2011CB808104). XQY would like to thank the support from the Alexander von Humboldt Foundation. TT is the holder of the Blaise Pascal chair of Ecole Normale Superieure.

* X.Yan@pku.edu.cn

† xthe@iapcm.ac.cn

- [1] S.V. Bulanov et al., Phys. Lett. A 299, 240 (2002); T. Zh. Esirkepov et al., Phys. Rev. Lett. 89, 175003 (2002).
- [2] M. Roth et al., Phys. Rev. Lett. 86, 436 (2001); V.Yu. Bychenkov et al., Plasma Phys. Rep. 27, 1017 (2001); S. Atzeni et al., Nucl. Fusion 42, L1 (2002).
- [3] K.W. D. Ledingham et al., J. Phys. D 36, L79 (2003); S.V. Bulanov et al., Plasma Phys. Rep. 30, 196 (2004).
- [4] J.W.Shearer et al., Phys. Rev. A 8, 1582 (1973).
- [5] S.C.Wilks et al., Phys. Plasma 8, 542 (2001).
- [6] <http://www.extreme-light-infrastructure.eu>.
- [7] A. Macchi, et al., Phys. Rev. Lett. 94, 165003 (2005);X. Zhang et al., Phys. Plasmas 14, 123108 (2007); X. Q. Yan, et al., Phys. Rev. Lett. 100, 135003 (2008); O. Klimo, et al., Phys. Rev. ST Accel. Beams 11, 031301 (2008); A. P. L. Robinson, et al., New J. Phys. 10, 013021 (2008); S. G. Rykovanov,et al., New J. Phys. 10, 113005 (2008); C. S. Liu,et al., AIP Conf. Proc. 1061, 246 (2008); A. Henig, et al.,Phys. Rev. Lett. 103, 245003 (2010).
- [8] X. Q. Yan, et al., Phys. Rev. Lett. 103, 135001 (2009).
- [9] Z. -M. Sheng, et al.,Phys. Plasmas 9, 3147 (2002).
- [10] T. Esirkepov, et al., Phys. Rev. Lett. 92, 175003 (2004).
- [11] B. Qiao, M. Zepf, M. Borghesi, and M. Geissler, Phys. Rev. Lett. 102, 145002;M. Chen, et al., Phys. Rev. Lett. 103, 024801 (2009); F. Pegoraro and S.V. Bulanov, Phys. Rev. Lett. 99, 065002 (2007);S. V. Bulanov et al.,Phys. Rev. Lett 104, 135003 (2010); Y. Yin, et al., Phys. Plasmas 15, 093106 (2008).
- [12] T. Tajima and J. M. Dawson,Phys. Rev. Lett. 43, 267 (1979); A. Pukhov and J. Meyer-ter-Vehn, Appl. Phys. B 74, 355 (2002);W. P. Leemans, et al., Nature Phys. 2, 696 (2006); W. Lu, et al., Phys. Rev. Lett. 96, 165002 (2006).
- [13] B.F. Shen,et al., Phys. Rev. Spec. Top. 12, 121301 (2009).
- [14] L. L. Yu, et al., New Journal of Physics 12 (2010) 045021.
- [15] E. Esarey and P. Sprangle, IEEE Trans. on Plasma Science, 24, 252 (1996); E. Esarey and M. Pilloff, Phys.

- Plasmas 2, 1432 (1995).
- [16] M. Ashour-Abdalla et al., Phys. Rev. A 23, 1906 (1981).
- [17] A. Caldwell, et al., Nat.Physics 5, 363 (2009).